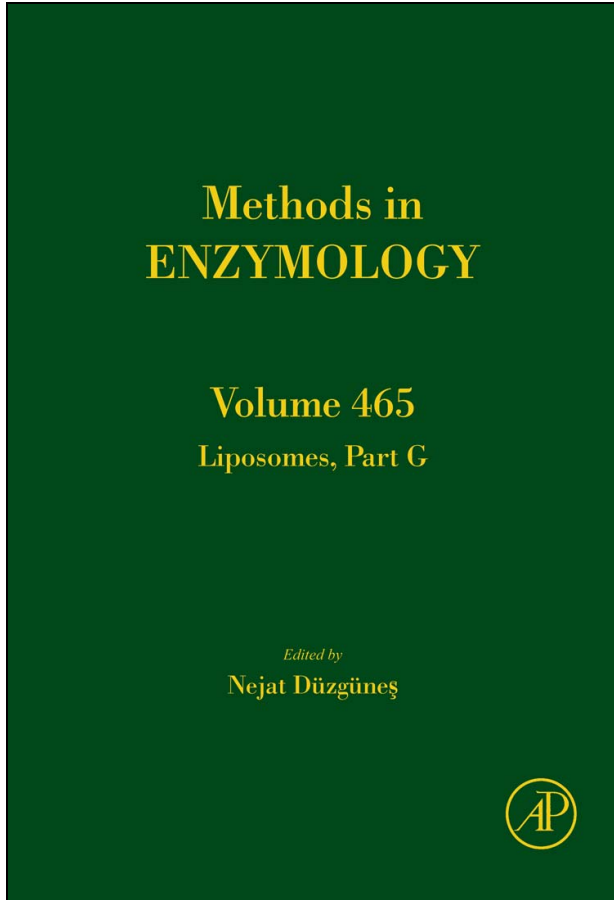


**Provided for non-commercial research and educational use only.
Not for reproduction, distribution or commercial use.**

This chapter was originally published in the book *Methods in Enzymology*, Vol. 465, published by Elsevier, and the attached copy is provided by Elsevier for the author's benefit and for the benefit of the author's institution, for non-commercial research and educational use including without limitation use in instruction at your institution, sending it to specific colleagues who know you, and providing a copy to your institution's administrator.



All other uses, reproduction and distribution, including without limitation commercial reprints, selling or licensing copies or access, or posting on open internet sites, your personal or institution's website or repository, are prohibited. For exceptions, permission may be sought for such use through Elsevier's permissions site at:

<http://www.elsevier.com/locate/permissionusematerial>

From: Mu-Ping Nieh, Norbert Kučerka, and John Katsaras, Spontaneously Formed Unilamellar Vesicles. In Nejat Düzgüneş, editor: *Methods in Enzymology*, Vol. 465, Burlington: Academic Press, 2009, pp. 3-20.

ISBN: 978-0-12-381379-4

© Copyright 2009 Elsevier Inc.

Academic Press.

SPONTANEOUSLY FORMED UNILAMELLAR VESICLES

Mu-Ping Nieh,^{*} Norbert Kučerka,^{*,†} and John Katsaras^{*,‡,§}

Contents

1. Introduction	4
2. Preparation of Spontaneously Forming ULVs	5
3. Characterization of ULVs	6
4. ULV Stability	7
5. Parameters Affecting ULVs	8
5.1. The path of formation	8
5.2. Charge density	8
5.3. The effect of long- to short-chain lipid molar ratios on morphology	10
5.4. Initial lipid concentration	11
5.5. Chain length of the long-chain lipid	11
5.6. Membrane rigidity	11
6. Mechanism of ULV Formation	12
7. Encapsulation and Controlled Release Mechanism of Spontaneously Formed ULVs	13
8. Application	16
9. Concluding Remarks	16
Acknowledgement	17
References	17

Abstract

Mixtures of long- and short-chain phospholipids can spontaneously form uniform unilamellar vesicles (ULVs) with diameters 50 nm (polydispersities of <0.3) or less. The morphology of these ULVs has mainly been characterized using small angle neutron scattering (SANS), a technique highly suited for the study of hydrogenous materials. Once formed, these ULVs have turned out to be highly stable and show great promise as imaging and therapeutic carriers.

^{*} Canadian Neutron Beam Centre, Steacie Institute for Molecular Sciences, Chalk River Laboratories, National Research Council Canada, Chalk River, Ontario, Canada

[†] Department of Physical Chemistry of Drugs, Faculty of Pharmacy, Comenius University, Bratislava, Slovakia

[‡] Department of Physics, Brock University, St. Catharines, Ontario, Canada

[§] Guelph-Waterloo Physics Institute and Biophysics Interdepartmental Group, University of Guelph, Guelph, Ontario, Canada

1. INTRODUCTION

Liposomes composed of phospholipids have proven to be highly effective in encapsulating therapeutic and diagnostic molecules (Hofheinz *et al.*, 2005; Zhang *et al.*, 2008), and for targeting specific sites of disease when functionalized with antibodies (Emerich and Thanos, 2007; Simone *et al.*, 2009; Torchilin, 2007). Liposomes possess many advantages including high loading capacities, the ability to entrap both hydrophilic and hydrophobic molecules, and biocompatibility (Lasic, 1998). The permeability of a phospholipid bilayer to small molecules is maximal at its phase-transition temperature, T_M (i.e., gel-to-liquid crystalline L_α phase), a desired condition for the release of encapsulated materials (Hays *et al.*, 2001; Inoue, 1974; Papahadjopoulos *et al.*, 1973; Yatvin *et al.*, 1978). There have been many studies devoted to controlling the transition temperature of liposomes through additives, such as cholesterol (Kraske and Mountcastle, 2001; Papahadjopoulos *et al.*, 1972; Sujatha and Mishra, 1998) and alcohols (McIntosh *et al.*, 1983; Rowe, 1983, 1985; Simon and McIntosh, 1984), to name a few.

Some zwitterionic phospholipids have a T_M within the physiological range of temperatures, but they naturally form large multilamellar vesicles (MLVs). Compared to unilamellar vesicles (ULVs), when introduced inside the human body they generally exhibit relatively short circulation half-lives, a property that can be controlled, for example, by varying the ULV size (Juliano and Stamp, 1975; Nabar and Nadkarni, 1998; Van Borssum Waalkes *et al.*, 1993; Zou *et al.*, 1995). ULVs have traditionally been formed from MLVs being sonicated or extruded through ceramic filters of specific pore size. Generally speaking, ULVs produced by sonication are polydisperse (different sizes), while extrusion methods, although capable of producing uniform size ULVs, is a labor intensive method that can be problematic for the production of small ULVs (<50 nm diameter) in quantities desired by industry, as the ceramic filters are easily fouled. As the size of ULVs is dictated by the filter's pore size, the smallest size ULVs that can routinely be produced by extrusion methods is ~ 40 nm in diameter. It is well known that ULVs larger than 50 nm in diameter have short circulation half-lives and tend to quickly accumulate in the liver and spleen (Allen *et al.*, 1989; Gregoriadis, 1995; Oku, 1999). Spontaneously formed ULVs provide the possibility of resolving some, or all of the aforementioned issues.

Self-assembled ULVs made of surfactants were first reported nearly two decades ago (Kaler *et al.*, 1989; Safran *et al.*, 1990; Talmon *et al.*, 1983). ULVs have been produced by mixing cationic and anionic surfactants (Iampietro and Kaler, 1999; Kaler *et al.*, 1992; Marques, 2000; Yatecilla *et al.*, 1996) through dilution (Caria and Khan, 1996; Demé *et al.*, 2002;

O'Connor *et al.*, 1997; Villeneuve *et al.*, 1999), and rapid changes in temperature (Lesieur *et al.*, 2000; Nieh *et al.*, 2001, 2004). However, the fact that the size of these ULVs was directly related to surfactant concentration (Bergström and Pedersen, 2000; Bergström *et al.*, 1999; Egelhaaf and Schurtenberger, 1999; Leng *et al.*, 2003; Oberdisse and Porte, 1997; Schurtenberger *et al.*, 1985) implied that leakage could be problematic during the fusion or fission of these ULVs. The use of these concentration-dependent ULVs is thus limited to situations where the environment, is, for the most part, reasonably stable. It was not until recently that we reported on a self-assembled ULV system composed entirely of phospholipids and whose size was independent of lipid concentration (Nieh *et al.*, 2003, 2004), greatly expanding the possible applications of ULVs. Over the years, we have conducted small angle neutron scattering (SANS) experiments to characterize the size and polydispersity of spontaneously forming ULVs, and found their average size to be less than 50 nm in diameter, with corresponding polydispersities of less than 0.3. It was also determined that their morphology is robust and not easily altered by additives (Nieh *et al.*, 2006). As a result, they can readily accommodate a range of amphiphilic molecules, making them highly desirable as contrast imaging and drug delivery vehicles. Importantly, the size of self-assembled ULVs can be controlled through the judicious use of long- to short-chain lipid mixing ratios, bilayer rigidity (e.g., inclusion of cholesterol), and charge density.

2. PREPARATION OF SPONTANEOUSLY FORMING ULVs

Generally speaking, spontaneously formed ULVs are composed of neutral long-chain [e.g., dimyristoyl phosphatidylcholine (di-14:0, DMPC); however, ditridecanoyl (di-13:0, DTPC) or dipalmitoyl phosphatidylcholine (di-16:0, DPPC) can also be used] and short-chain [e.g., dihexanoyl phosphatidylcholine (di-6:0, DHPC)] lipids, and a long-chain charged lipid (e.g., dimyristoyl phosphatidylglycerol, DMPG). A mixture of DMPC/DHPC/DMPG (e.g., molar ratio of 3.2:1:0.04) dissolves in water (or appropriate buffer) with an initial total lipid concentration of 20 wt% through successive vortexing and temperature cycling between 4 and 60 °C, until the solution is transparent at 4 °C. The transparent solution can then be progressively diluted to 10, 5, and finally 2.0 wt% total lipid concentration, keeping in mind to vortex and temperature cycle at each lipid concentration. It is important that the 2 wt% sample be kept at 4 °C prior to any further dilution, and then only diluted with 4 °C water. The morphology at these low-total lipid concentrations is one of the bilayered micelles (commonly known as bicelles), which transform into small monodisperse ULVs at temperatures >40 °C, as was determined by small angle neutron scattering (SANS) (Nieh *et al.*, 2003, 2004).

3. CHARACTERIZATION OF ULVs

ULVs are best characterized using a combination of dynamic light scattering (DLS) and small angle X-ray or neutron scattering (SAXS or SANS). For example, DLS can provide information regarding the hydrodynamic radius, R_H , which in addition, includes all of the water molecules attached to the ULV, and is calculated from the diffusion of ULVs using the Stokes–Einstein relation, keeping in mind that it is possible for a small molecule to have a larger hydrodynamic radius than a large molecule if it is surrounded by a greater number of solvent molecules (Nieh *et al.*, 2004). However, the structure of ULVs is more precisely obtained through SANS (Nieh *et al.*, 2001, 2002) or SAXS (Lesieur *et al.*, 2000; Weiss *et al.*, 2005). Normally, SANS (or SAXS) data are plotted as a function of scattered intensity, I , versus scattering vector, q [$= (4\pi/\lambda) \sin(\theta/2)$, where λ and θ are the wavelength and the scattering angle, respectively]. The probing range of length scales thus lies between $2\pi/q_{\min}$ and $2\pi/q_{\max}$, where q_{\min} and q_{\max} are the attainable minimum and maximum q values, in the case of SANS typically between 0.003 and 0.5 \AA^{-1} (i.e., between 2000 and 10 \AA). With this sensitivity, SANS is ideally suited in determining the diameter (not the hydrodynamic radius as obtained from DLS) and shell thickness of ULVs.

Figure 1.1 illustrates typical SANS data arising from a low-polydispersity ULV sample using the 30 m SANS instrument located at the National Institute of Standards and Technology (NIST, USA) Center for Neutron

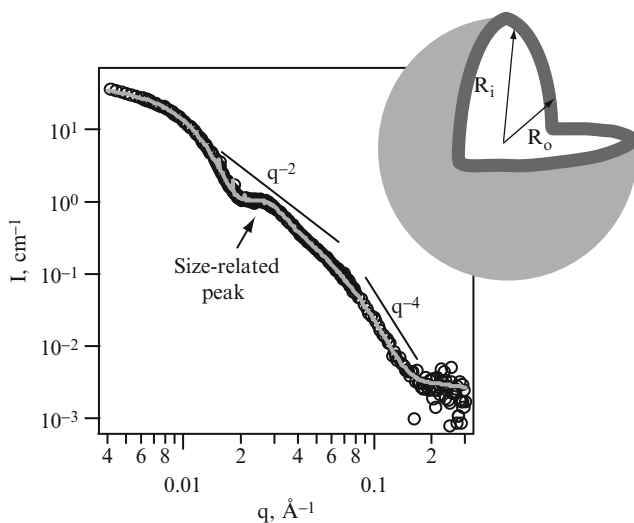


Figure 1.1 Typical SANS data of low-polydispersity ULVs (circles) and the best-fit curve (gray line) using the depicted spherical shell model.

Research (NCNR). The data are best fitted through the use of a polydisperse spherical shell model, as described in Eq. (1.1) (Feigin and Svergun, 1987) using the IGOR Pro software[®]. The data fitting procedure was developed by the NCNR (Kline, 2006).

SANS scattered intensity can be written as follows:

$$I_{\text{vesicle}}(q) = \frac{\phi_{\text{vesicle}}}{V_{\text{vesicle}}} \int_0^{\infty} f(r) A_o^2(qr) dr, \quad (1.1)$$

where ϕ_{vesicle} and V_{vesicle} are the total volume fraction of ULVs, and the total volume occupied by an individual ULV, respectively. The amplitude of the form factor (spherical shell model), $A_o(qr)$, is given as

$$A_o(qr) = \frac{4\pi(\rho_{\text{lipid}} - \rho_{\text{solvent}})}{q^3} \left[\left(\sin q \frac{R_i}{R_o} r - \sin qr \right) - qr \left(\frac{R_i}{R_o} \cos q \frac{R_i}{R_o} r - \cos qr \right) \right]$$

$$f(r) = \frac{(p^{-2/p^2})(r/\langle R_o \rangle)^{(1-p^2)/p^2} e^{-r/(p^2 \langle R_o \rangle)}}{\langle R_o \rangle \Gamma(1/p^2)},$$

where R_i , R_o , ρ_{lipid} and ρ_{solvent} are the inner and outer ULV radii, and the coherent neutron scattering length densities of the lipid and the solvent, respectively. $f(r)$ is the Schulz distribution function describing the size distribution of ULV radii and p is the polydispersity of R_o , which is defined as $\sigma/\langle R_o \rangle$, where σ^2 is the variance of R_o . $\langle R_o \rangle$ represents the average R_o . The scattering pattern from small, uniform ULVs generally exhibits the following two features when plotted on a log-log graph (Fig. 1.1):

1. SANS data at q less than ~ 0.01 (\AA^{-1}) reveal the average ULV size (also known as the “Guinier” regime), while data at q greater than ~ 0.01 (\AA^{-1})—excluding oscillations—follow a q^{-2} dependence, indicative of a planar structure (i.e., the ULV’s shell). At the high q regime ($q > 0.1$ \AA^{-1}), the intensity exhibits a q^{-4} dependence corresponding to the interfacial scattering from the lipid bilayer (Porod’s law).
2. The broad peak appearing along the SANS curve ($q \sim 0.25$ \AA^{-1} in Fig. 1.1) is a measure of ULV size, while the number of oscillations is a good indicator of the range of ULV sizes (i.e., more oscillations translate to a narrower size distribution or low polydispersity).

4. ULV STABILITY

One important characteristic of a system’s suitability as a potential drug delivery carrier is its stability under variable conditions, for example, changes in concentration and/or temperature. As mentioned, although

surfactant-based self-assembled ULVs can exhibit low polydispersities (Oberdisse and Porte, 1997; Schurtenberger *et al.*, 1985), their size is for the most part, concentration dependent, with ULV fusion and fission taking place with changes in total surfactant concentration. Table 1.1 shows that spontaneously formed ULVs are extremely stable when they are diluted at a temperature of 45 °C and exhibit polydispersities ranging from 0.15 to 0.23 (Nieh *et al.*, 2003)—it is believed that the small decrease in ULV radii after 2 weeks is due to lipid degradation.

5. PARAMETERS AFFECTING ULVs

5.1. The path of formation

Phase diagrams of DMPC/DMPG/DHPC phospholipid mixtures have previously been constructed (Katsaras *et al.*, 2005; Nieh *et al.*, 2004; Yue *et al.*, 2005), as shown in Figure 1.2. From these phase diagrams it is clear that ULVs exist at temperatures ≥ 35 °C and at lipid concentrations ≤ 1.25 wt%. Moreover, it was determined that low-polydispersity ULVs could only be formed from low temperature monodisperse bicelles, whereby DMPC undergoes a gel to the liquid crystalline (L_α) phase transition. Importantly, it is believed that bicelles dictate ULV size (discussed in a later section)—diluting a high-concentration lipid mixture at a temperature beyond DMPC's T_M results in polydisperse ULVs (Nieh *et al.*, 2005).

5.2. Charge density

Charge density plays an important role in the formation of spontaneously formed ULVs. Figure 1.3 shows SANS data from three lipid mixtures with different charge densities, R (defined as $[\text{DMPG}]/[\text{DMPC}]$) of 0, 0.01, and 0.67, respectively. ULVs were found to form at $R = 0.01$. In the case of the neutral system, the spherical shell model was able to describe most of data except for the peak at $\sim 0.1 \text{ \AA}^{-1}$, a signature of DMPC MLVs (Hui and He, 1983; Janiak *et al.*, 1976), thus implying the coexistence of ULVs and MLVs. As for the highly charged lipid mixture ($R = 0.067$), the bilayered micelle morphology persisted throughout the temperature range studied (Nieh *et al.*, 2002).

These results demonstrate that there is an optimal charge density for the formation of ULVs, and that the different morphologies are highly dependent on the delicate balance of interactions between membrane fluctuations and the various Coulombic repulsive, van der Waal, and hydration forces (Pozo-Navas *et al.*, 2003).

Table 1.1 ULV $\langle R_o \rangle$ and polydispersities as a function of lipid concentration at 45 °C

Lipid concentration	1.0 wt%		0.5 wt%		0.25 wt%
	5 h	5 h	4 days	2 weeks	5 h
$\langle R_o \rangle$ (Å)	378 ± 20	378 ± 15	382 ± 25	332 ± 20	363 ± 15
Polydispersity (p)	0.23 ± 0.10	0.16 ± 0.05	0.15 ± 0.05	0.19 ± 0.08	0.22 ± 0.08

1 wt% samples were diluted at room temperature.

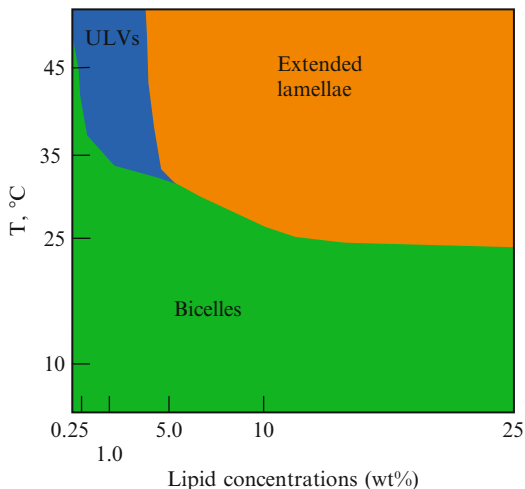


Figure 1.2 Structural phase diagram constructed by SANS.

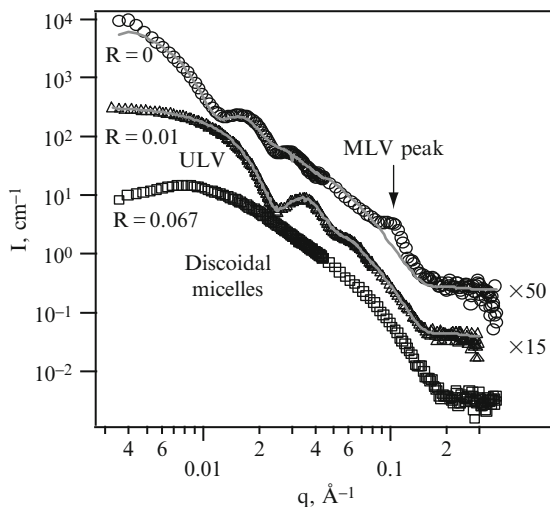


Figure 1.3 SANS data from mixtures of 0.25 wt% DMPC/DHPC/DMPG at 45 °C, and R ($[DMPG]/[DMPC]$) equal 0 (circles), 0.01 (triangles), and 0.067 (squares). The gray lines are best-fits to the data using the spherical shell model form factor.

5.3. The effect of long- to short-chain lipid molar ratios on morphology

The effect of Q ($=[DMPC]/[DHPC]$) on ULV size has been studied by Nieh *et al.* (to be published). Over a Q range between 2.5 and 4, all ULVs exhibited relatively low polydispersities (i.e., $0.23 \leq p \leq 0.31$), with the

Table 1.2 $\langle R_i \rangle$ and ULV polydispersities as a function of Q

Long- to short-chain lipid molar ratio (Q)	$\langle R_i \rangle$ (Å)	Polydispersity (p)
2.5	190	0.31
3.0	168	0.28
3.5	133	0.26
4.0	117	0.23

average ULV R_i decreasing from 190 to 117 Å (Table 1.2). This Q dependence of ULV radii is believed to be highly correlated with bicelle size, from which ULVs are formed. At higher Q values, because there are insufficient amounts of DHPC coating the bicelle rim, bicelles fold into ULVs earlier, resulting in much smaller ULVs.

5.4. Initial lipid concentration

As was mentioned, concentration-independent spontaneously formed ULVs were diluted at room temperature; however, their final size was found to vary depending on the path of formation. For example, it is known that ULV size strongly depends on initial total lipid concentration at low temperatures where bicelles are present. Increasing temperature resulted in the formation of ULVs with $\langle R_i \rangle$ of ~ 180 and ~ 80 Å for total lipid concentrations of 1.0 and 0.1 wt%, respectively (Nieh *et al.*, 2008). Once formed, the size of these ULVs was not affected by further dilutions (Nieh *et al.*, 2003). An important note is that bicelle size (i.e., bicelle concentration) dictates ULV size.

5.5. Chain length of the long-chain lipid

DMPC is the most commonly used long-chain phospholipid in preparing spontaneously formed ULVs. However, the longer chain lipid DPPC or the shorter DTPC can be used instead of DMPC to form low-polydispersity ULVs. The average ULV size for $Q = 3.2$ and 0.1 wt% lipid concentration decreased slightly as a function of increasing chain length, that is, $\langle R_i \rangle = 112, 97,$ and 95 Å in the case of DTPC, DMPC, and DPPC, respectively (to be published). This dependence can be rationalized in the manner by which bicelles fold onto themselves to form ULVs (see later section).

5.6. Membrane rigidity

It is well known that cholesterol increases membrane rigidity (Boggs and Hsia, 1972; Mendelsohn, 1972). Cholesterol was used to modify the rigidity of bicelles from which highly stable ULVs can be obtained up to a cholesterol concentration of 20 mol%. Preliminary SANS data also indicates that

Table 1.3 Parameters affecting the size of self-assembled ULVs

Parameters	Effects
Path	Polydispersity
Charge density	Lamellarity
Q, long- to short-chain molar ratio	--
Initial lipid concentration	++
Chain length of long-chain lipid	-
Membrane rigidity	+

The symbols “+” and “-” represent increasing or decreasing ULV size, respectively. Their numbers are an indicator of their intensity.

$\langle R_i \rangle$ of spontaneously formed ULVs increases with increasing cholesterol content (to be published). Table 1.3 summarizes the various parameters studied. It seems that initial lipid concentration and [DMPC]/[DHPC] molar ratio have the most profound effect on ULV size, affecting $\langle R_i \rangle$ by more than 100%. However, besides the parameters listed in Table 1.3, another important factor that may affect ULV size is the solution's salinity (Yue *et al.*, 2005).

6. MECHANISM OF ULV FORMATION

There are a few theories purporting to explain the formation of spontaneously formed ULVs. These include a negative modulus of Gaussian curvature as a result of charged bilayers (Winterhalter and Helfrich, 1992), a nonzero spontaneous curvature from the unequal distribution of the two molecular species making up the inner and outer bilayer leaflets (Safran *et al.*, 1991), a calculation based on a molecular thermodynamics model (Yuet and Blankschtein, 1996), and a kinetically trapped model of disk-like micelles transforming into vesicles (Leng *et al.*, 2003). However, experimental support for these various theories is mostly based on particular systems, where formation mechanisms can vary greatly. For the most part, the results discussed in this chapter are best described by the model proposed by Fromherz (1983), whereby the transformation of bicelles to ULVs is driven by the line tension at the bicelle's rim (shown in Fig. 1.4).

Bicelles at low temperature are thought to have the long-chain DMPC lipid residing in their planar region and the short-chain DHPC lipid predominantly located at their rim—thus minimizing the energy penalty arising from the high curvature at the disk's rim and possible exposure of DMPC's hydrophobic chains to water. Segregation between the two lipid species is most likely the direct result of their immiscibility, as DMPC is in the gel phase and DHPC is in the L_α phase. Around 24 °C, DMPC's acyl

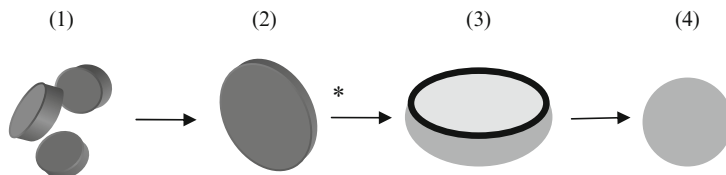


Figure 1.4 Proposed mechanism for the formation of monodisperse spontaneously formed ULVs from bicelles. For the most part, it is believed that DHPC molecules populate the bicelle's rim, while DMPC are found in the bicelle's planar region, see [Fromherz \(1983\)](#).

chains melt resulting in its increased miscibility with DHPC. As a result, some of the DHPC partitions into the bicelle's DMPC-rich planar region causing the rim's line tension to increase. At some point, when enough DHPC has partitioned into the bicelle's planar region, in order to prevent the bicelle's hydrophobic core from becoming exposed to water, the bicelles fuse forming larger bicelles. At some point (yet to be understood), the larger bicelles begin to fold, at first forming a bowl and eventually a hollow sphere (ULV).

The proposed model suggests that the ULV size-determining stage is when the larger bicelles begin to fold. This implies that a more flexible membrane should yield smaller ULVs consistent with what was observed in the case of cholesterol-doped systems. However, membrane flexibility is not the only factor influencing ULV size. Another key factor is bicelle stability, whereby more stable bicelles can have more time to interact and coalesce with neighboring bicelles. This is reflected by the fact that larger ULVs were formed at lower Q values, as bicelles are more stable with higher amounts of DHPC. Nevertheless, the fact that different long-chain lipids resulted in a small decrease in ULV size—as their hydrocarbon chain length was increased (i.e., DTPC, DMPC, and DPPC)—can be rationalized as follows: Longer hydrocarbon chains translate into stiffer bilayers and higher transition temperatures stabilizing the bicelle morphology. On the other hand, in the case of thicker bilayers (i.e., longer chain lipids), more DHPC is required to stabilize the bicelles; therefore, for a given concentration of DHPC the bicelles cannot grow as large and fold into small ULVs. It therefore seems that these competing effects practically cancel each other out, resulting in no dramatic change to the size of ULVs.

7. ENCAPSULATION AND CONTROLLED RELEASE MECHANISM OF SPONTANEOUSLY FORMED ULVs

The encapsulation and leakage properties of spontaneously formed ULVs were studied using fluorescence spectroscopy ([Nieh *et al.*, 2008](#)). Two ULV mixtures (0.2 and 1.0 wt%) were prepared at 4 °C in an aqueous

solution containing 12.5 mM of the fluorescent probe 8-aminonaphthalene-1,3,8-trisulfonic disodium salt (ANTS), and 45 mM of the fluorescence quencher *p*-xylene-bis-pyridinium bromide (DPX). If both the fluorescent probe and quencher are in close proximity (i.e., confined within an individual ULV), there is practically no fluorescence. After encapsulation, freely floating fluorescent probes and quenchers were removed from the solution at 45 °C using a PD-10 size-exclusion chromatography (SEC) column containing SephadexTM G-25. Triton X-100, an agent commonly used to compromise vesicle structure was added to the eluted ULVs, forcing them to release their contents and the resultant fluorescence was monitored. When ULVs leak or break apart—reducing the probability of the quencher interacting with the fluorescent probe—fluorescence intensity dramatically increases. Figure 1.5 shows the fluorescence response of 1 wt% ULVs at 10 and 45 °C upon the addition of Triton X-100. From the 45 °C data it is clear that ULVs (as determined by SANS) encapsulate both fluorescent probe and quencher; this is not, however, the case for bicelles (10 °C).

The 0.2-wt% ULV sample at 45 °C (Fig. 1.6) behaves in a similar manner (Fig. 1.5). However, unlike the 1 wt% sample, some degree of encapsulation is retained, even at 10 °C. This result is supported by SANS data, whereby it was observed that at low lipid concentrations ULV do not form bilayered micelles. Instead, they deform into ellipsoidal vesicles (Nieh *et al.*, 2005), thus maintaining a certain degree of encapsulating capability.

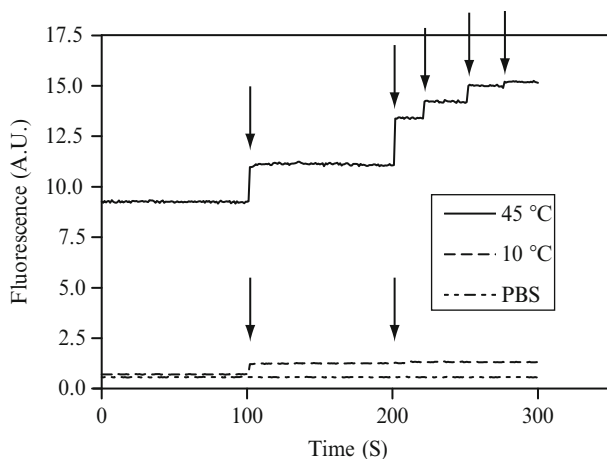


Figure 1.5 Fluorescence response of a 1.0 wt% DMPC/DHPC/DMPG mixture at 45 °C (solid line) and 10 °C (dashed line), and PBS buffer only (broken line). The arrows represent the addition of Triton X-100. Increase in fluorescence intensity is the result of ULVs (45 °C) being compromised, thus releasing fluorescent probe and quencher molecules. For further details, see Nieh *et al.* (2008).

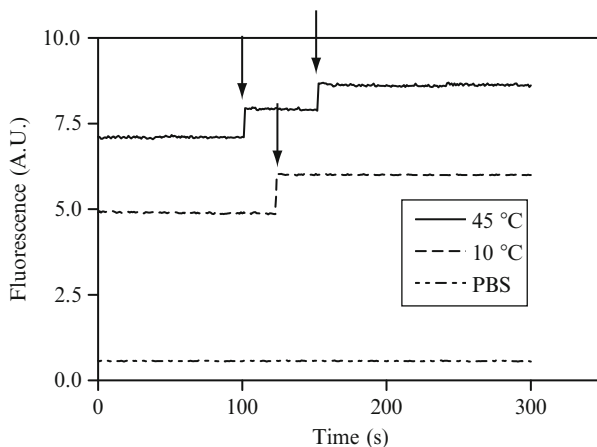


Figure 1.6 Fluorescent response of a 0.2 wt% DMPC/DHPC/DMPG mixture at 45 °C (solid line) and 10 °C (dashed line), and PBS buffer only (broken line). The arrows represent the addition of Triton X-100. Increase in fluorescence intensity is due to ULVs (45 °C) or ellipsoidal vesicles (10 °C) being compromised, thus releasing fluorescent probe and quencher molecules. For further details see [Nieh *et al.* \(2008\)](#).

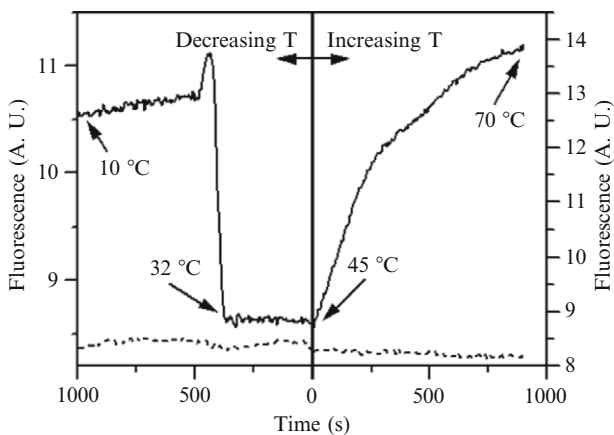


Figure 1.7 Fluorescence response of 1.0 wt% ULVs (solid line) and PBS buffer only (broken line), upon heating and cooling. Two ULV samples were prepared at 45 °C (0 s), one was cooled, while the other was heated.

It is also known that self-assembled ULVs composed of DMPC/DHPC/DMPG exhibit two temperature-dependent release mechanisms. [Figure 1.7](#) shows that between 32 and 45 °C, ULVs are highly stable. However, beyond 45 °C they begin to leak and continue to do so at temperatures up to 70 °C, albeit at a different rate. On the other hand, at a temperature

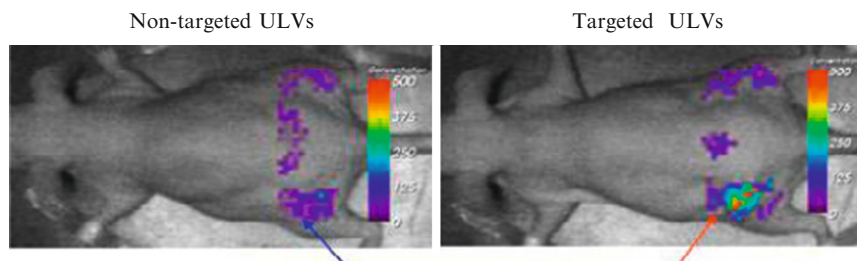


Figure 1.8 Imaging payloads delivered to a xenograft tumor using antibody-functionalized ULVs loaded with Gd, Cy5.5, and the C225 antibody. The Cy5.5 signal is predominant in the tumor where functionalized ULVs were used.

below 32 °C, ULVs transform into bicelles, releasing their contents. At elevated temperatures, it is thought that ULVs begin to leak at an increasing rate because of lipid flip-flop taking place between the inner and outer bilayer leaflets.

8. APPLICATION

Recently, spontaneously formed ULVs have been reformulated to target and image disease (Abulrob *et al.* 2009). The ULVs were modified as follows: (a) functionalized PEGylated lipids (i.e., distearoyl PC-polyethylene glycol (PEG)-maleimide) was incorporated, onto which a targeting molecule (i.e., C225 single domain antibody) was attached; (b) DMPC was replaced with a magnetic resonance imaging (MRI) contrast agent [i.e., gadolinium (Gd)-diethylenetriamine pentaacetic acid (DTPA)-2-benzoxazolinone (BOA)]; and (c) di-18:1 dodecylamine phosphatidylethanolamine was added to conjugate the near-infrared probe, Cy 5.5.

For the *in vivo* study, the human glioblastoma cell line (U87MG) that expresses the epidermal growth factor receptor (EGFR) was injected into the flank of nude mice and allowed to develop a tumor over a period of 10 days. Disease targeted and nontargeted ULVs were then injected into animals, which were imaged 24 h after injection. Significant accumulation of Cy5.5 in the xenograft tumor was detected only in the case of the targeted ULV formulation (Fig. 1.8).

9. CONCLUDING REMARKS

Treatment of disease can involve surgery and/or therapies, including radiation, chemo and hormonal and biological therapies. In the course of these treatments, healthy tissues can be damaged, resulting in unwanted side

effects. However, the use of drugs specifically targeted to a disease can minimize the toxic side effects associated with many conventional therapies (e.g., chemotherapy). Low polydispersity, spontaneously formed ULVs show great promise in enhancing the efficacy of various medical imaging techniques (e.g., MRI and positron emission tomography) and drug treatments (e.g., cancers and diseases of the brain). The features that make them attractive for commercialization are as follows: (1) they are inexpensive, made up exclusively of low-cost phospholipids; (2) their size and polydispersity can be controlled; (3) they are highly stable, providing long shelf-life and extended circulation half-lives when inserted into the body; and (4) the ULV preparation is easily adaptable to industrial scale production. The latter two features are distinct advantages over lipid-based ULVs produced by traditional extrusion and sonication methods. Preliminary *in vivo* experiments show that these ULVs can be fabricated to both target and image diseased tissues.

ACKNOWLEDGEMENT

NK would like to acknowledge funding from the Advanced Foods and Materials Network, part of the Networks of Centres of Excellence.

REFERENCES

- Abulrob, A., Stanimirovic, D., Iqbal, U., Nieh, M.-P., and Katsaras, J. (2009). *Single domain antibody-targeted carrier for contrast agents and drug delivery agents* US Provisional Patent 61/228,117.
- Allen, T. M., Hansen, C., and Rutledge, J. (1989). Liposomes with prolonged circulation times: Factors affecting uptake by reticuloendothelial and other tissues. *Biochim. Biophys. Acta* **981**, 27–35.
- Bergstrom, M., and Pedersen, J. S. (2000). A small-angle neutron scattering study of surfactant aggregates formed in aqueous mixtures of sodium dodecyl sulfate and didodecyldimethylammonium bromide. *J. Phys. Chem. B* **104**, 4155–4163.
- Bergstrom, M., Pedersen, J. S., Schurtenberg, P., and Egelhaaf, S. U. (1999). Small-angle neutron scattering (SANS) study of vesicles and lamellar sheets formed from mixtures of an anionic and a cationic surfactant. *J. Phys. Chem. B* **103**, 9888–9897.
- Boggs, J. M., and Hsia, J. C. (1972). Effect of cholesterol and water on the rigidity and order of phosphatidylcholine bilayers. *Biochim. Biophys. Acta* **290**, 32–42.
- Caria, A., and Khan, A. (1996). Phase behavior of catanionic surfactant mixtures: Sodium bis (2-ethylhexyl)sulfosuccinate–didodecyldimethylammonium bromide–water system. *Langmuir* **12**, 6282–6290.
- Demé, B., Dubois, M., Gulik-Krzywicki, T., and Zemb, T. (2002). Giant collective fluctuations of charged membranes at the lamellar-to-vesicle unbinding transition. 1. Characterization of a new lipid morphology by SANS, SAXS, and electron microscopy. *Langmuir* **18**, 997–1004.
- Egelhaaf, S. U., and Schurtenberger, P. (1999). Micelle-to-vesicle transition: A time-resolved structural study. *Phys. Rev. Lett.* **82**, 2804–2807.

- Emerich, D. F., and Thanos, C. G. (2007). Targeted nanoparticle-based drug delivery and diagnosis. *J. Drug Target.* **15**, 163–183.
- Feigin, L. A., and Svergun, D. I. (1987). Determination of the integral parameters of particles. In *Structure Analysis by Small Angle X-Ray and Neutron Scattering* pp. 59–105. Plenum Press, New York.
- Fomherz, P. (1983). Lipid-vesicle structure: Size control by edge-active agents. *Chem. Phys. Lett.* **94**, 259–266.
- Gregoriadis, G. (1995). Engineering liposomes for drug delivery. *Trends Biotechnol.* **13**, 527–537.
- Hays, L. M., Crowe, J. H., Wolkers, W., and Rudenko, S. (2001). Factors affecting leakage of trapped solutes from phospholipid vesicles during thermotropic phase transitions. *Cryobiology* **42**, 88–102.
- Hofheinz, R.-D., Gnad-Vogt, S. U., Beyer, U., and Hochhaus, A. (2005). Liposomal encapsulated anti-cancer drugs. *Anticancer Drugs* **16**, 691–707.
- Hui, S. W., and He, N. B. (1983). Molecular organization in cholesterol-lecithin bilayers by X-ray and electron diffraction measurements. *Biochemistry* **22**, 1159–1164.
- Iampietro, D. J., and Kaler, E. W. (1999). Phase behavior and microstructure of aqueous mixtures of cetyltrimethylammonium bromide and sodium perfluorohexanoate. *Langmuir* **15**, 8590–8601.
- Inoue, K. (1974). Permeability properties of liposomes prepared from dipalmitoyllecithin, dimyristoyllecithin, egg lecithin, rat liver lecithin and beef brain sphingomyelin. *Biochim. Biophys. Acta* **339**, 390–402.
- Janiak, M. J., Small, D. M., and Shipley, G. G. (1976). Nature of the thermal pretransition of synthetic phospholipids: Dimyristoyl- and dipalmitoyllecithin. *Biochemistry* **15**, 4575–4580.
- Juliano, R. L., and Stamp, D. (1975). The effect of particle size and charge on the clearance rates of liposomes and liposome encapsulated drugs. *Biochem. Biophys. Res. Commun.* **63**, 651–658.
- Kaler, E. W., Murthy, A. K., Rodrigues, B. E., and Zasadzinski, J. A. N. (1989). Spontaneous vesicle formation in aqueous mixtures of single-tailed surfactant. *Science* **245**, 1371–1374.
- Kaler, E. W., Herrington, K. L., Murthy, A. K., and Zasadzinski, J. A. N. (1992). Phase behavior and structures of mixtures of anionic and cationic surfactants. *J. Phys. Chem.* **96**, 6698–6707.
- Katsaras, J., Harroun, T. A., Pencer, J., and Nieh, M.-P. (2005). “Bicellar” lipid mixtures as used in biochemical and biophysical studies. *Naturwissenschaften* **92**, 355–366.
- Kline, S. R. (2006). Reduction and analysis of SANS and USANS data using IGOR Pro. *J. Appl. Crystallogr.* **39**, 895–900.
- Kraske, W. V., and Mountcastle, D. B. (2001). Effects of cholesterol and temperature on the permeability of dimyristoylphosphatidylcholine bilayers near the chain melting phase transition. *Biochim. Biophys. Acta* **1514**, 159–164.
- Lasic, D. D. (1998). Novel application of liposomes. *Trends Biotechnol.* **16**, 307–321.
- Leng, J., Egelhaaf, S. U., and Cates, M. E. (2003). Kinetics of micelle-to-vesicle transition: Aqueous lecithin-bile salt mixtures. *Biophys. J.* **85**, 1624–1646.
- Lesieur, P., Kiselev, M. A., Barsukov, L. I., and Lombardo, D. (2000). Temperature-induced micelle to vesicle transition: Kinetic effects in DMPC/NaC system. *J. Appl. Crystallogr.* **33**, 623–627.
- Marques, E. F. (2000). Size and stability of catanionic vesicles: Effects of formation path, sonication and aging. *Langmuir* **16**, 4798–4807.
- McIntosh, T. J., McDaniel, R. V., and Simon, S. A. (1983). Induction of an interdigitated gel phase in fully hydrated phosphatidylcholine bilayers. *Biochim. Biophys. Acta* **731**, 109–114.

- Mendelsohn, R. (1972). Laser-Raman spectroscopic study of egg lecithin and egg lecithin-cholesterol mixtures. *Biochim Biophys. Acta* **290**, 15–21.
- Nabar, S. J., and Nadkarni, G. D. (1998). Effect of size and charge of liposomes on biodistribution of encapsulated ^{99m}Tc -DTPA in rats. *Indian J. Pharmacol.* **30**, 199–202.
- Nieh, M.-P., Glinka, C. J., Krueger, S., Prosser, R. S., and Katsaras, J. (2001). SANS study of structural phases of magnetically alignable lanthanide-doped phospholipid mixtures. *Langmuir* **17**, 2629–2638.
- Nieh, M.-P., Glinka, C. J., Krueger, S., Prosser, S. R., and Katsaras, J. (2002). SANS study on the effect of lanthanide ions and charged lipids on the morphology of phospholipid mixtures. *Biophys. J.* **82**, 2487–2498.
- Nieh, M.-P., Harroun, T. A., Raghunathan, V. A., Glinka, C. J., and Katsaras, J. (2003). Concentration-independent spontaneously forming biomimetic vesicles. *Phys. Rev. Lett.* **91**, 1581051–1581054.
- Nieh, M.-P., Harroun, T. A., Raghunathan, V. A., Glinka, C. J., and Katsaras, J. (2004). Spontaneously formed monodisperse biomimetic unilamellar vesicles: The effect of charge, dilution, and time. *Biophys. J.* **86**, 2615–2629.
- Nieh, M.-P., Raghunathan, V. A., Kline, S. R., Harroun, T. A., Huang, C.-Y., Pencer, J., and Katsaras, J. (2005). Spontaneously formed unilamellar vesicles with path-dependent size distribution. *Langmuir* **21**, 6656–6661.
- Nieh, M.-P., Pencer, J., Katsaras, J., and Qi, X. (2006). Spontaneously forming ellipsoidal phospholipid unilamellar vesicles and their interactions with helical domains of saposin C. *Langmuir* **22**, 11028–11033.
- Nieh, M.-P., Katsaras, J., and Qi, X. (2008). Controlled release mechanisms of spontaneously forming unilamellar vesicles. *Biochim. Biophys. Acta* **1778**, 1467–1471.
- Oberdisse, J., and Porte, G. (1997). Size of microvesicles from charged surfactant bilayers: Neutron scattering data compared to an electrostatic model. *Phys. Rev. E* **56**, 1965–1975.
- O'Connor, A. J., Hatton, T. A., and Bose, A. (1997). Dynamics of micelle-vesicle transitions in aqueous anionic/cationic surfactant mixtures. *Langmuir* **13**, 6931–6940.
- Oku, N. (1999). Delivery of contrast agents for positron emission tomography imaging by liposomes. *Adv. Drug. Deliv. Rev.* **37**, 53–61.
- Papahadjopoulos, D., Nir, S., and Ohki, S. (1972). Permeability properties of phospholipid membranes: Effect of cholesterol and temperature. *Biochim. Biophys. Acta* **266**, 561–583.
- Papahadjopoulos, D., Jacobson, K., Nir, S., and Isac, T. (1973). Phase transitions in phospholipid vesicles: Fluorescent polarization and permeability measurements concerning the effect of temperature and cholesterol. *Biochim. Biophys. Acta* **311**, 330–348.
- Pozo-Navas, B., Raghunathan, V. A., Katsaras, J., Rappolt, M., Lohner, K., and Pabst, G. (2003). Discontinuous unbinding of lipid bilayers. *Phys. Rev. Lett.* **91**, 028101.
- Rowe, E. S. (1983). Lipid chain length and temperature dependence of ethanol-phosphatidylcholine interactions. *Biochemistry* **22**, 3299–3305.
- Rowe, E. S. (1985). Thermodynamic reversibility of phase transitions specific effects of alcohols on phosphatidylcholine. *Biochem. Biophys. Acta* **813**, 321–330.
- Safran, S. A., Pincus, P., and Andelman, D. (1990). Theory of spontaneous vesicle formation in surfactant mixtures. *Science* **248**, 354–356.
- Safran, S. A., Pincus, P., Andelman, D., and MacKintosh, F. C. (1991). Stability and phase behavior of mixed surfactant vesicles. *Phys. Rev. A* **43**, 1071–1078.
- Schurtenburger, P., Mazer, N., and Kanzig, W. (1985). Micelle-to-vesicle transition in aqueous solutions of bile salt and phosphatidylcholine. *J. Phys. Chem.* **89**, 1042–1049.
- Simon, S. A., and McIntosh, T. J. (1984). Interdigitated hydrocarbon chain packing causes the biphasic transition behavior in lipid/alcohol suspensions. *Biochim. Biophys. Acta* **773**, 169–172.
- Simone, E., Ding, B.-S., and Muzykantov, V. (2009). Targeted delivery of therapeutics to endothelium. *Cell Tissue Res.* **335**, 283–300.

- Sujatha, J., and Mishra, A. K. (1998). Phase transitions in phospholipid vesicles: Excited state prototropism of 1-naphthol as a novel probe concept. *Langmuir* **14**, 2256–2262.
- Talmon, Y., Evans, D. F., and Ninham, B. W. (1983). Spontaneous vesicles formed from hydroxide surfactants: Evidence from electron microscopy. *Science* **221**, 1047–1048.
- Torchilin, V. P. (2007). Targeted pharmaceutical nanocarriers for cancer therapy and imaging. *AAPS J.* **9**, E128–E147.
- Van Borssum Waalkes, M., Kuipers, F., Havinga, R., and Scherphof, G. L. (1993). Conversion of liposomal 5-fluoro-2'-deoxyuridine and its dipalmitoyl derivative to bile acid conjugates of α -fluoro- β -alanine and their excretion into rat bile. *Biochim. Biophys. Acta* **1176**, 43–50.
- Villeneuve, M., Kaneshina, S., Imae, T., and Aratono, M. (1999). Vesicle-micelle equilibrium of anionic and cationic surfactant mixture studied by surface tension. *Langmuir* **15**, 2029–2036.
- Weiss, T. M., Narayanan, T., Wolf, C., Gradzielski, M., Panine, P., Finet, S., and Helsby, W. I. (2005). Dynamics of self-assembly of unilamellar vesicles. *Phys. Rev. Lett.* **94**, 038303.
- Winterhalter, M., and Helfrich, W. (1992). Bending elasticity of electrically charged bilayers: Coupled monolayers, neutral surfaces and balancing stresses. *J. Phys. Chem.* **96**, 327–330.
- Yatcilla, M. T., Herrington, K. L., Brasher, L. L., Kaler, E. W., Chiruvolu, S., and Zasadzinski, J. A. N. (1996). Phase behavior of aqueous mixtures of cetyltrimethylammonium bromide (CTAB) and sodium octyl sulfate (SOS). *J. Phys. Chem.* **100**, 5874–5879.
- Yatvin, M. B., Weinstein, J. N., Dennis, W. H., and Blumenthal, R. (1978). Design of liposomes for enhanced local release of drugs by hyperthermia. *Science* **202**, 1290–1293.
- Yue, B., Huang, C.-Y., Nieh, M.-P., Glinka, C. J., and Katsaras, J. (2005). Highly stable phospholipid unilamellar vesicles from spontaneous vesiculation: A DLS and SANS study. *J. Phys. Chem. B* **109**, 609–616.
- Yuet, P. K., and Blankschtein, D. (1996). Molecular-thermodynamic modeling of mixed cationic/anionic vesicles. *Langmuir* **12**, 3802–3818.
- Zhang, L., Gu, F. X., Chan, J. M., Wang, A. Z., Langer, R. S., and Farokhzad, O. C. (2008). Nanoparticles in medicine: Therapeutic applications and developments. *Clin. Pharmacol. Ther.* **83**, 761–769.
- Zou, Y., Lin, Y.-H., Reddy, S., Priebe, W., and Perez-Soler, R. (1995). Effect of vesicle size and lipid composition on the in vivo tumor selectivity and toxicity of the non-cross-resistant anthracycline annamycin incorporated in liposomes. *Int. J. Cancer* **61**, 666–671.